



Faculty of Electrical Engineering and  
Information Technology STU in Bratislava

**Anna Kálosi**

Dissertation Thesis Abstract

**Preparation and Research of Functionalized MoS<sub>2</sub>  
based Nanoplatfrom for Biomedical Application**

Reg. No. FEI-104400-87870

to obtain the Academic Title of „philosophiae doctor”,  
abbreviated as „PhD.“)

in the doctorate degree study programme: Physical Engineering

in the field of study: Electrical and Electronics Engineering

Form of Study: full-time

in Bratislava, 2020



**Dissertation Thesis has been prepared at**  
Slovak Academy of Sciences, Institute of Physics, Department of  
Multilayers and Nanostructures

**Submitter:** Anna Kálosi  
Slovak Academy of Sciences, Institute of Physics,  
Department of Multilayers and Nanostructures  
Dúbravská cesta 9, Bratislava

**Supervisor:** RNDr. Eva Majková, DrSc.  
Slovak Academy of Sciences, Institute of Physics,  
Department of Multilayers and Nanostructures  
Dúbravská cesta 9, Bratislava

**Consultant:** Dr. Rer. Nat. Peter Siffalovič, PhD.  
Slovak Academy of Sciences, Institute of Physics,  
Department of Multilayers and Nanostructures  
Dúbravská cesta 9, Bratislava

**Readers:**

**Dissertation Thesis Abstract was sent**

**Dissertation Thesis Defence will be held at**

prof. Dr. Ing. Miloš Oravec  
dekan FEI STU



Fakulta elektrotechniky a informatiky  
STU v Bratislave

**Anna Kálosi**

Autoreferát dizertačnej práce

**Príprava a výskum funkcionalizovanej  
nanoplatformy na báze MoS<sub>2</sub>  
pre biomedicínsku aplikáciu**

Reg. No. FEI-104400-87870

na získanie akademického titulu „doktor“,  
v skratke „PhD.“)

v doktorandskom študijnom programe: fyzikálne inžinierstvo

v študijnom odbore: elektrotechnika

Forma štúdia: denná prezenčná

in Bratislava, 2020

**Dizertačná práca bola vypracovaná na**

Fyzikálny ústav Slovenskej akadémie vied, Oddelenie multivrstiev a nanoštruktúr

**Predkladateľ:** Anna Kálosi

Fyzikálny ústav Slovenskej akadémie vied  
Oddelenie multivrstiev a nanoštruktúr  
Dúbravská cesta 9, Bratislava

**Školiteľ:** RNDr. Eva Majková, DrSc.

Fyzikálny ústav Slovenskej akadémie vied  
Oddelenie multivrstiev a nanoštruktúr  
Dúbravská cesta 9, Bratislava

**Konzultant:** Dr. Rer. Nat. Peter Siffalovič, PhD.

Fyzikálny ústav Slovenskej akadémie vied  
Oddelenie multivrstiev a nanoštruktúr  
Dúbravská cesta 9, Bratislava

**Oponenti:**

**Autoreferát bol rozoslaný**

**Obhajoba dizertačnej práce sa bude konať dňa**

prof. Dr. Ing. Miloš Oravec

dekan FEI STU

## Contents

Contents.....	5
Abstract.....	6
Abstrakt .....	7
PhD Assignment.....	8
Introduction .....	10
Methods.....	15
Results and discussion .....	21
Conclusion .....	28
List of publications.....	30
Bibliography.....	33

## Abstract

This work aims to further develop a 2D transition metal dichalcogenide based nanoplatform for cancer detection and treatment system. Following the PhD dissertation objectives, The PhD thesis contains the state of the art of MoS<sub>2</sub> exfoliation and deposition, functionalization of the surface of MoS<sub>2</sub> nanosheets to design a cancer detection and treatment nanoplatform, testing the cell-nanoparticle interaction on selected cell lines. It discusses a planar test platform that models the behavior of the nanoplatform via in situ imaging ellipsometry. Furthermore, it shows and discusses the internalization of a MoS<sub>2</sub> nanoplatform in vitro with the prospect of achieving high selectivity towards cancerous cells using Raman imaging, confocal laser scanning microscopy, and flow cytometry measurements.

## Abstrakt

Cieľom tejto práce je ďalej rozvinúť nanoplatformu založenú na 2D dichalgenidov prechodových kovov na design systému cieleného dodávania liekov a detekcie nádorových buniek. V súlade s cieľmi dizertácie, táto práca primárne obsahuje súčasný stav techniky MoS<sub>2</sub> exfoliacie a depozície, funkcionalizáciu povrchu MoS<sub>2</sub> nanovrstiev pre vytvorenie nanoplatformy pre detekciu a liečbu rakovinových buniek, ďalej testovanie interakcie nanoplatformy s vybranými rakovinovými bunkami. Diskutuje planárnu testovaciu platformu na modelovanie nanoplatformy s použitím zobrazovacej elipsometrie. Ďalej prezentuje internalizáciu nanoplatformy MoS<sub>2</sub> in vitro s perspektívou dosiahnutia vysokej selektivity voči rakovinovým bunkám pomocou Ramanovho konfokálneho zobrazovania, prietokovej cytometrie a konfokálnym fluorescenčným skenovacím mikroskopom.



# PhD Assignment

Slovak University of Technology in Bratislava  
Institute of Nuclear and Physical Engineering

Faculty of Electrical Engineering and Information Technology  
Academic year: 2018/2019  
Reg. No.: FEI-104400-87870



## DISSERTATION THESIS TOPIC

Student: **Ing. Anna Kálosi**  
Student's ID: 87870  
Study programme: Physical Engineering  
Study field: Electrical and Electronics Engineering  
Thesis supervisor: RNDr. Eva Majková, DrSc.  
Consultant: Dr.Rer.Nat. Peter Šíffalovič, PhD.  
Workplace: Institute of Physics of the Slovak Academy of Sciences

Topic: **Preparation and Research of Functionalized MoS<sub>2</sub> based Nanoplatfom for Biomedical Application**

Language of thesis: English

Specification of Assignment:

The aim of the dissertation is to research the physical properties of functionalized nanomaterials (MoS<sub>2</sub>) with a focus on the field of biomedicine and theranostics.

1st year

Selection of suitable types of MoS<sub>2</sub> nanosheets in terms of lateral dimensions and number of layers for functionalization by biomolecules for potential treatment of cancer cells. Preparation of Langmuir layer from MoS<sub>2</sub> nanolayers and deposition on a planar substrate to monitor the functionalization of the nanosheets with molecules by imaging ellipsometry Evaluation of experiments, preparation of publications and presentations at domestic and international conferences.

2nd year

Implementation of the dynamic in situ experiments based on imaging ellipsometry using a microfluidic cell to monitor the functionalization process of MoS<sub>2</sub> nanosheets. Usage of complementary methods, e.g. AFM, learning the principles of Raman microscopy. Evaluation of experiments, preparation of publications and presentations at domestic and international conferences. Writing the rigorous thesis, passing the dissertation exam.

3rd year

Studies of the interaction of a functionalized nanoplatfom with cells using Raman confocal microscopy. Study of the penetration of the nanoplatfom across the cell membrane as well as the agglomeration inside the cell. Evaluation of experiments, preparation of publications and presentations at domestic and international conferences. Writing the dissertation thesis and defense.



Assignment procedure from: 06. 09. 2016

Date of thesis submission: 31. 05. 2019

**Ing. Anna Káloš**  
Solver

**prof. Ing. Vladimír Nečas, PhD.**  
Head of department

**prof. Ing. Julius Círák, CSc.**  
Study programme supervisor

## Introduction

Low-dimensional nanomaterials as potential drug delivery and treatment agents were in the spotlight during the last decade. Nanomaterials for the theranostic and biomedical applications can be synthesized from different types of materials (e.g. gold nanoparticles [1] and other metals [2], 2D materials [3], polymers [4]). Tailoring the size [5] and shape [6], [7] of these nanomaterials affects the efficiency of the drug delivery and cellular uptake. Besides factors like shape, size, and size-dispersion, researchers tried to control the surface chemistry of the nanomaterials (e.g. coatings to prevent opsonization [8], [9] or active targeting with peptides [10], antibodies [11]–[13], etc.).

After the discovery of graphene [14], the research was focused also on other 2D materials as well. Several derivatives of graphene were introduced as new nominees for targeted drug delivery systems, these were graphene oxide (GO) and reduced graphene oxide (rGO) [15], [16]. As the research of 2D materials broadened, parameters of 2D TMDs [17] predicted potential biomedical applications as well, e.g. as a functionalized nanoplatform for cancer detection and treatment [18], especially after Chou et al. [19] showed that MoS<sub>2</sub> nanosheets have better photothermal performance than graphene, different approaches of photothermal therapy were demonstrated [20]–[23].

In the bulk form, the metal atom layer of MoS<sub>2</sub> is surrounded by two layers of the chalcogen atoms, creating a sandwich-like structure kept together by van der Waals forces. The exfoliation process overcomes these weak forces and reduces the material thickness up to few-layer MoS<sub>2</sub> nanosheets. At present, the

## ::::STU

solvent-assisted liquid phase exfoliation [24] is widely applied as a low cost and up-scalable method for the preparation of MoS<sub>2</sub> nanosheets. The application of different solvents has been reported [24]–[31], the N-methyl-2-pyrrolidone (NMP) being the most effective one [31]. During the last years, the possibility of the MoS<sub>2</sub> liquid exfoliation in the polar solvents with low boiling point, such as water, has been studied [32], several successful approaches have been published, such as sonication at elevated temperatures [33], the addition of a small amount of ammonia [34], mechanical thinning of the precursor [35], reduction of the lateral size of the precursor [36].

The MoS<sub>2</sub> nanosheets possess an exceptionally high surface to volume ratio, making them an outstanding candidate for treatment and drug delivery systems. These systems require large space for surface interactions on a small scale. The defect sites of MoS<sub>2</sub> can be used to accomplish surface functionalization, typically, by binding sulfur-containing ligands (thiols) to them [37]. The most common defect states of the exfoliated MoS<sub>2</sub> nanosheets are the sulfur vacancies both on the edges and on the surface of the nanosheet [38]. The sulfur atoms are used to fill up the vacancies thus enabling basal plane ligand conjugation. One of the most frequently described candidates for the surface functionalization for biomedical application is polyethylene glycol (PEG) molecule terminated with lipoic acid (LA). The lipoic acid contains the sulfur necessary to fill up the vacancies on the nanosheet. In the article by Liu et al. [39], it was reported that lipoic acid conjugated PEG containing a disulfide group at the PEG terminal enables strong binding to MoS<sub>2</sub> and the PEG enhances the physiological stability of the MoS<sub>2</sub>. Furthermore, Liu et al. in an article [23] showed that the PEG not

# STU

only stabilizes the MoS<sub>2</sub> solution but also increases the cellular uptake of the PEG-MoS<sub>2</sub> sheets.

Considering these findings, the nanoplatform model that my PhD research was devoted to study, consists of a MoS<sub>2</sub> nanosheet base, functionalized covalently with lipoic acid (LA) terminated PEG. This PEGylated platform needs to be able to bind the proper antibodies that can bind to cancer cells. Therefore, this nanoplatform design uses a PEG molecule that has on one terminal the lipoic acid on the other terminal the biotin. Biotin is a water-soluble vitamin that can be bonded to avidin (avidin is a glycoprotein which has a very high affinity to bind biotin). The avidin-biotin non-covalent bond has high specificity and strength, it is widely used in biological sciences [40], [41]. Moreover, one avidin can bind up to four biotins and biotin can be conjugated to several different molecules, this feature allows to introduce biotinylated molecules, antibodies, cytotoxins, fluorescent dyes, etc. to the system. Biotinylation process (conjugation of biotin to other proteins, molecules) is a well-known and already described technique [42] and it allows us to immobilize biotinylated antibodies on MoS<sub>2</sub>-LA-PEG-biotin nanoplatform through a biotin-avidin-biotin bridge. The immobilization process through this biotin-avidin-biotin bridge was described before as a potential technique useful for drug screening, diagnostics, and biosensor applications by Sundberg et al [43], thence it was used for instance for immobilization of DNA [44], or proteins [45], etc.

Combining the above-described knowledge and methods, the complete form of the cancer detection and treatment nanoplatform is MoS<sub>2</sub> – LA-PEG-biotin – avidin – biotinylated

# STU

antibody. As it is apparent, the production steps of these nanoplatform follow the sequence: exfoliation MoS<sub>2</sub>, PEGylation through lipoic acid with a PEG that has both LA and biotin on its terminals, subsequent exposition of the MoS<sub>2</sub>-LA-PEG-biotin to avidin, then binding of the biotinylated antibodies.

The choice of the antibody bioconjugated to the nanoplatform was made in cooperation with the Institute of Virology (Biomedical Research Center of the Slovak Academy of Sciences). Researchers in this institute (Pastoreková et al.) identified previously the CAIX (carbonic anhydrase IX) protein (initially named as MN-protein) in HeLa human cervical carcinoma cell line [46], [47]. CAIX is an enzyme in the CA family, these enzymes catalyze the production of proton and bicarbonate from carbon dioxide and water [48]. CAIX is expressed mostly in carcinomas, in any forms of cancer, not in normal tissue [49]. It was also shown that the CAIX is dependent on the density of the cells, and it is activated under stressful conditions such as hypoxia (deprivation of oxygen from the tissue) [50]. The anti-human carbonic anhydrase IX (M75) is a recombinant monoclonal antibody to CAIX. Because the CAIX is a biomarker for many cancerous cells, the nanoplatform bioconjugated to M75 would be able to connect to CAIX expressing cells. Both the biotinylated antibody and the CAIX expressing cell lines in my study are provided by the group of Pastoreková.

In my PhD thesis I am providing answers to several questions that needed to be addressed during my research. First question concerns the MoS<sub>2</sub> nanoflakes, to be able to utilize the MoS<sub>2</sub> nanoflakes, the selection of the MoS<sub>2</sub> nanoflakes is to be addressed: Which method is capable of producing high quality

# ::::STU

flakes with narrow band of size dispersion in means of lateral size and thickness as well? Is this method also reliable, can it be up scaled for larger production in the future?

The second question to address is the ability of these MoS<sub>2</sub> flakes to be functionalized – How should be the MoS<sub>2</sub> functionalized? Which material to use to make sure that the platform is non-toxic for the in vitro experiments and the later for in vivo usage? How to verify the functioning of the functionalization? How to bond the antibodies to the platform?

The third question concerns the situation when the platform is properly functionalized, the antibodies are already bonded to the system: How to verify that the uptake of the nanoplatfroms into the cells is done?

The fourth question is: How to track the processes on cellular level and how to quantify the ratios of internalized nanoplatfroms inside target cells, vs. control cells?

In this Dissertation Thesis Abstract, I am presenting my main results. These results were also already published at the beginning of 2020 in an article [51].

## Methods

### Additive-free MoS<sub>2</sub> liquid phase exfoliation

The exfoliation of bulk MoS<sub>2</sub> powder was performed in deionized water (DI) with two subsequent sonication and centrifugation steps without a previous precursor treatment. The MoS<sub>2</sub> exfoliation started with the powder MoS<sub>2</sub> (Alfa Aesar) dispersed in 10 ml deionized ultrapure water. The MoS<sub>2</sub> dispersion was stirred on a laboratory shaker, then 10 ml of DI was added and sonicated in an ultrasonic bath (Sonorex RK 510 H, Bandelin) at a temperature of 10°C for 24 hours. Afterward, the solution was centrifuged for 20 min with RCF 21.000 g (Model 3-30K, Sigma centrifuge) at 20°C. The supernatant was collected by micropipette and the precipitate was dissolved again in 20 ml of DI water, sonicated again for 24 h and centrifuged in the same manner as before. The sample was collected by micropipette and then stored at 6°C in a refrigerator unit.

### Planar test platform

Silicon wafers with native oxide (approximately 2 nm thick SiO<sub>2</sub>) were used as substrates. Before the deposition, the substrates were cleaned (subsequently acetone, isopropyl, and DI water using an ultrasonic bath, then the substrates were dried with nitrogen). The next step was the preparation of the Langmuir film. For this purpose, a slightly modified Langmuir Schaefer deposition method was used. The Langmuir Blodgett (LB) trough (KSV NIMA-HC) was filled with DI water, pH modified with HCl to achieve better surface spreading of the MoS<sub>2</sub> flakes. For the LB deposition, LPE in ethanol nanoflakes were used [26]. The substrates were placed under the water with a slightly tilted

# STU

angle. The flakes were dropped onto the water surface using a burette. The burette was set to deliver MoS<sub>2</sub> solution drops onto the surface until the surface pressure reached 5mN/m, then the trough was left 30 to complete the flake spreading process. Afterward, the LB trough was set to the least possible speed that the apparatus allows compressing the surface layer. The process stops when the closed packed monolayers of MoS<sub>2</sub> flakes is reached, around 23 mN/m [26]. After the compression was finished the extraction of the subphase took place, then the substrates were left to dry.

In the next step, LA-PEG-biotin was dispersed in DI water, the substrates with MoS<sub>2</sub> monolayer were placed into the solution then the beaker was placed in a laboratory mixer and left overnight on low shake intensity. On the other end of the LA-PEG-biotin, the biotin should be ready to bind avidin in the next step.

## **Avidin-biotin formation via ellipsometry**

The formation of the avidin-biotin complex was confirmed via ellipsometry. The Accurion imaging type ellipsometer was complemented with a microfluidic cell and a liquid handling system.

The design of the experiment was the following:

- 4 liquids were placed to the reservoirs of the liquid handling system, DI water, phosphate-buffered saline (PBS), bovine serum albumin (BSA) in PBS, avidin in PBS;
- BSA was chosen as a control protein, that should not bind to the biotinylated surface;

# STU

- the functionalized substrate was placed into the microfluidic cell, and the cell was filled with DI water;
- the arms of the ellipsometer were adjusted to 60° than the cell was aligned, and the light was focused on the substrate surface;
- when the adjustments were done the cell was filled with PBS and the liquid sequence was adjusted using the user-interface of the ellipsometry software (5 min PBS, 15 min BSA, 35 min avidin, 5 min PBS);
- the ellipsometer was set to measure psi and delta at a single wavelength of 549.1 nm once in every minute;
- the peristaltic pump was started together with the ellipsometry measurement.

## **Nanoplatfom in solution**

After the exfoliation in DI water, the MoS<sub>2</sub> nanosheets were covered with LA terminated PEG (LA-PEG-biotin, MW 2000, Nanocs). In the next step avidin (160 kDa, 0,98 µg/µl, GBiosciences) was bind on to the biotin terminal. We used biotinylated anti-human carbonic anhydrase IX (M75) [52].

After each step, dialysis filtering was used to dispose of the excess material that did not bound to our nanoplatfom. After the PEGylation with 2000 kDa PEG, we used a dialysis membrane of MWCO 12 kDa (Standard RC Tubing Spectra/Por®2, SpectrumLabs), after the addition of avidin 300 kDa, after bio-conjugation of the M75 antibody 1000 kDa.

**Viability assay**

Conventional viability testing was performed on exfoliated MoS<sub>2</sub> nanosheets, on PEGylated MoS<sub>2</sub> and M75 conjugated nanoplateforms on JIMT-1 and MRC5 cell lines. The protocol for the cell maintenance was the following: One hundred thousand JIMT-1 and MRC5 cells per well were seeded on 96-well plate and incubated in a humidified atmosphere at 37°C in the presence of 5% CO<sub>2</sub>. Then, the nanoplateforms were incubated in hypoxia with cells for 24 and 48 hours. After the incubation, 20 µl/well of CellTiter-Blue solution (CellTiter-Blue Viability assay kit, Promega) was added and incubated at 37°C for 1 hour. The fluorescence was measured on the Synergy HT microreader (Bio-Tek) at Ex530/Em590. The average fluorescence and standard deviation were obtained from three parallel replicas for each sample.

**Flow cytometry assay**

The statistical behavior of the nanoplateform internalization was analyzed with the flow cytometer Guava® easyCyte Plus (Millipore) with an excitation wavelength of 488 nm. The interaction between CAIX and M75 was demonstrated with JIMT-1 breast carcinoma, as a typical example of CAIX expressing cancer cell line. As a negative control, MRC5 fibroblasts were used.

One hundred thousand JIMT-1 and MRC5 cells per well were seeded on 96-well plate and incubated in a humidified atmosphere at 37°C in the presence of 5% CO<sub>2</sub> in a similar manner as in case of the viability assay. The next day cells were

# STU

moved to hypoxia workstation (Invivo300, Ruskinn) with 1% O<sub>2</sub> and 5% CO<sub>2</sub> atmosphere for 24 hours to induce CAIX protein expression. Nanoplatfoms were incubated with donkey anti-mouse IgG (H+L) secondary antibody conjugated with fluorescent tag Alexa Fluor 488 (Thermo Fisher Scientific) in 1:1000 dilution for 1 hour at 37°C on a rotation shaker. After 24 hours of incubation in hypoxia, the labeled nanoplatfoms (30 µl/well) were added to the cells and incubated for 3, 6, and 24 hours. After the indicated time, the cells were washed with PBS and trypsinized. Detached cells were centrifuged at 800 rpm for 5 min and washed with PBS. 200 µl of cell suspension was analyzed on Guava easyCyte plus cytometer. The average absorbance and standard deviation were obtained from parallel replicas for each sample.

## **Confocal Raman microscopy**

800 thousand cells were seeded on a coverslip in a Petri dish. The cells (JIMT-1 an MRC5) were incubated under hypoxic conditions for 24 h followed by adding 500 µl/dish of the unlabeled nanoplatfom. After 24 hours, the cells were washed and imaging was performed in physiological solution (pH=7.4, Oxoid) by a confocal Raman microscopy (CRM, Alpha300 R+, WITec) using an immersion objective (W Plan-Apochromat 63x, NA=1, Zeiss, Germany). The cells were scanned with 532 nm laser (Spectra-Physics Excelsior 532-60). The spectroscopic data were collected by a spectrophotometer (UHTS 300, WITec) equipped with a 600 g/mm grating (blazed at 500 nm) coupled to an EMCCD camera (Newton DU970N-BV-353, Andor).

## ::::STU

The datasets measured on each cell were processed by the Witec CRM software. First, the cosmic ray removal and principal component analysis (PCA) was done, followed by k-means clustering. The MoS<sub>2</sub> is detectable by the two main modes, the E<sub>2g</sub><sup>1</sup> (in-plane vibrations, 383 cm<sup>-1</sup>) and A<sub>1g</sub> (out-of-plane vibrations, 407 cm<sup>-1</sup>) [53]. The stretching modes of water (3051 cm<sup>-1</sup>, 3233 cm<sup>-1</sup>, 3393 cm<sup>-1</sup>, 3511 cm<sup>-1</sup>, 3628 cm<sup>-1</sup>) [54] are observed in the intra- and extra-cellular regions, while the asymmetric CH<sub>2</sub> stretch mode (2854 cm<sup>-1</sup>) of lipids, fatty acids, and proteins together with the symmetric CH<sub>3</sub> stretch mode (2930 cm<sup>-1</sup>) of proteins are indicators of the intracellular regions of the confocal Raman image [55]–[57].

## Results and discussion

### Planar test platform

The samples exposed to the LA-PEG-biotin solution were analyzed with X-ray photoelectron spectroscopy (XPS) which confirmed that the deposition was successful.

The results of the ellipsometry experiment are shown in Fig. 1 [58], it is apparent that the  $\psi$  and  $\Delta$  are not changing when PBS or BSA are introduced to the system, but after the cell is filled with avidin solution, the  $\Delta$  shows a clear change. Considering the nature of such thin layers, it was expected that only the phase shift ( $\Delta$ ) changes and the amplitude ratio ( $\tan(\psi)$ ) remain unchanged. The three different sets of points correspond to three different regions of interest measured on the CCD camera on the same sample.

The *in situ* experiment with the ellipsometer confirmed that one can functionalize the surface of  $\text{MoS}_2$  by binding the LA-PEG-biotin molecule to the surface. The biotin stays active on the surface, and it can form a biotin-avidin complex after exposure to avidin. Since an avidin or streptavidin molecule can bind exactly four biotins, it opens up the possibility to attach another biotinylated molecule to the platform.

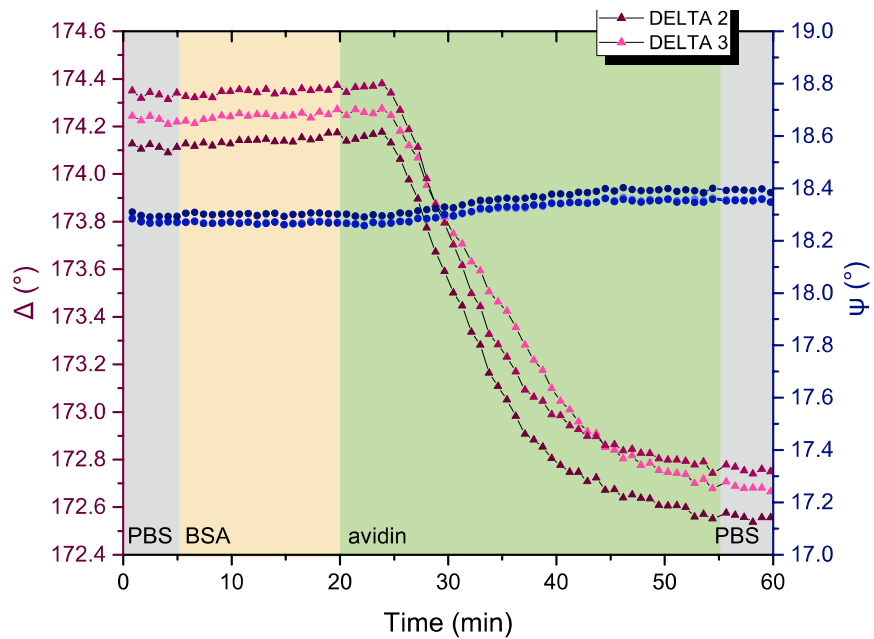


Figure 1 - Time-resolved in situ ellipsometric measurements of the formation of an avidin layer on biotinylated MoS<sub>2</sub> surface.

# STU

## Viability

The *in vitro* cell viability was evaluated on the exfoliated MoS<sub>2</sub> nanosheets, PEGylated MoS<sub>2</sub> nanosheets. The observed fluorescence was normalized to the fluorescence measured on the control plates both in the case of the JIMT-1 breast carcinoma cells and the MRC5 fibroblasts. The fluorescence did not cause any critical damage neither to the cancer cells nor to the healthy ones after the 24 h and 48 h exposures.

Our results were in agreement with previously published results of *in vitro* cytotoxicity assessment evaluating 2D chemically exfoliated MoS<sub>2</sub> [59] and PEGylated MoS<sub>2</sub> [39]. These articles considered the 2D nanosheets essentially nontoxic or only with low cytotoxicity. The research of Chng et al. [60] pointed out that the viability measurements displayed stronger toxicity with the increasing density of nanosheets exfoliated with methyllithium, n-butyllithium, and tert-butyllithium. Appel et al.[61] found the methyllithium exfoliated MoS<sub>2</sub> nanosheets were biocompatible and non-mutagenic for their tested cell line. Unlike these studies, there is neither intercalating material nor other solvent and/or additive during the LPE in our case that can affect the results of the viability assay.

In the paper by Zhu et al. [62], the viability of cancerous HeLa and MCF7 breast cells incubated with MoS<sub>2</sub> nanosheets reached almost 100%. Feng et al[20] used 4T1 breast cancer cells. They stated that no significant cytotoxicity was observed after 24 h and 48 h incubation of the cells with PEGylated MoS<sub>2</sub> nanosheets at any concentration. Jia et al.[63] showed that HeLa cells incubated 24 h with MoS<sub>2</sub> had 100% of viability. Bare MoS<sub>2</sub> nanosheets exfoliated similarly to our method in water were examined by Kaur et al.[64] on different cancerous and healthy

## STU

cell lines (MCF7 breast cancer, U937 leukemia, HaCaT keratinocyte cell line), observing evident cytotoxicity in the case of leukemia cells. Unlike the cell lines studied by Kaur et al. [64], the fluorescence did not show impaired cell viability in JIMT-1 and MRC5 cells studied by us. Each type of tumor exhibits different responses upon internalization. It is also apparent from the above-mentioned studies that the viability is strongly affected by the method of exfoliation, in particular by the solvent used. Therefore, no general conclusions on the interaction between cells and MoS<sub>2</sub> nanosheets can be adopted.

### **Flow cytometry**

The flow cytometer is capable of counting the fluorescent-labeled cells from a mixed cell population based on the light scattering and fluorescence of the investigated cells [65]. In our study, we used it to determine the number of cells interacting with the antibody conjugated MoS<sub>2</sub> based nanoplatform. The measurements quantified the number of cells, giving us a better understanding of the probability of such interaction.

The results showed in Fig. 3 confirm that the CAIX expressing JIMT-1 cells incorporated more nanoplatforms after 6 and 24 h incubation time than the control MRC5 cells without the CAIX expression. The greatest difference of 30 % between JIMT-1 and MRC5 cells was observed after 24 h incubation time. However, what flow cytometry measures are the portion of the cells interacting with the nanoplatforms. This interaction firstly happens on the cell membrane, when the CAIX and M75 are binding one to another. Therefore, the information from the flow cytometry measurement does not validate the completion of the internalization process, overestimating the ratio of internalized

# STU

nanoplatfroms. For this reason, we followed up with the inspection of the cells by confocal Raman microscopy.

## **Confocal Raman Microscopy**

The confocal Raman microscopy is a label-free technique providing information on the localization of the nanoplatfrom in a cell [66]–[68]. The identified cellular compartments and MoS<sub>2</sub> nanoplatfroms together with the decomposed Raman spectra at three different cross-sections are shown in Fig. 2A-C and Fig. 2D-F, respectively [51]. The increased tryptophan signal at 750 cm<sup>-1</sup> suggests lysosome activity in certain subcellular areas. In particular, this is apparent in Fig. 4C. The tryptophan signal was also detectable in the case of MRC5 cells around the nanoplatfroms.

Some types of antibodies can induce receptor-antibody mediated internalization upon their binding. Most applications of monoclonal antibodies in cancer therapy utilize this specific way of import, where the antibody-receptor complexes are trapped in early endosomes, then they either degrade or recycle to the cell surface [66]. However, in our case we can exclude this type of internalization, as the M75 antibody is not able to induce this type of cell endocytosis [67]. by Zhu et al. [62], it was proposed that possible three endocytosis pathways are involved in MoS<sub>2</sub> internalization: clathrin-mediated endocytosis, endocytosis mediated by caveolin, and macropinocytosis. They stated, that the most common pathway in HeLa and MCF-7 cell lines was the caveolae-dependent pathway. However, the cells used also the clathrin-dependent pathway and macropinocytosis. The healthy human aortic endothelial cells (HAOEC) preferred the caveolae-dependent pathway and also macropinocytosis [62]. Most likely,

# STU

our cells (JIMT-1 and MRC5) utilize the same pathways for MoS<sub>2</sub> nanosheet internalization as reported by Zhu et al.

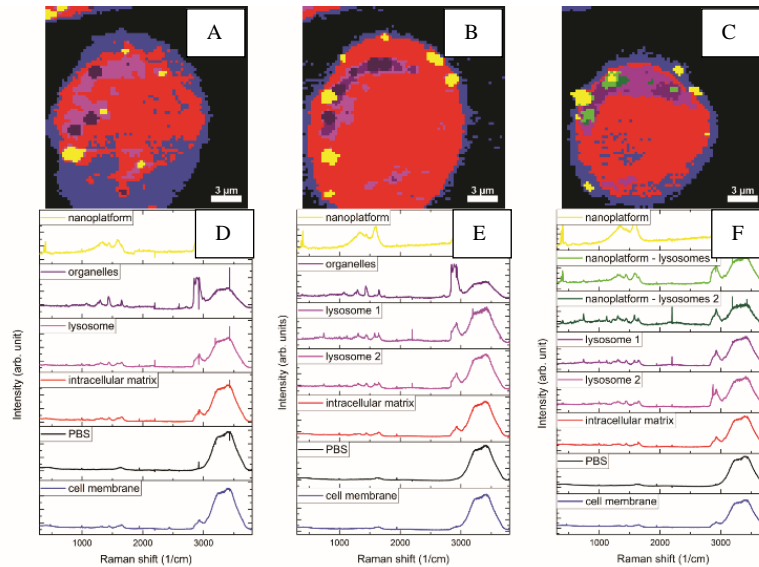


Figure 2 - Label-free Raman localization of MoS<sub>2</sub> nanoplateforms (sample MP2-M75) in JIMT-1 cell. Reconstructed false color images at A) z = 0 μm, B) z = 2 μm, and C) z = 4 μm. The corresponding Raman spectra (D-F) below each image have the same color codes (phosphate buffer saline - black, cell membrane - blue, intracellular matrix - red, lysosomes and organelles - purple shades, MoS<sub>2</sub> nanoplateform - yellow, nanoplateform with clear lysosome peak - green).

## Conclusion

In conclusion, my PhD research is aiming towards a biomedical, theranostic application of MoS<sub>2</sub>. In this Dissertation Thesis Abstract, I focused on the main result of my research, summarized the motivation for the research in the section Introduction, and presented the design of the nanoplatforms that I studied. My research focused on the understanding of the fundamental aspects of the interaction between cells and nanoplatforms, mainly the efficiency of such interaction and the development of a protocol to increase the efficiency towards selected cell types. The results of the in vitro localization of the nanoplatforms and on the efficiency of the antigen-antibody based recognition element are shown in section Results and discussion.

Employing this antigen-antibody binding, we increased the probability of the MoS<sub>2</sub> nanosheet endocytosis into CAIX expressing cells (JIMT-1) by 30%. The nanosheets are functionalized by a specific antibody M75, which forms an antigen-antibody complex with CAIX. The cellular internalization was quantified by flow cytometry, while the internalization was confirmed on the sub-micrometer scale in vitro by label-free confocal Raman imaging. The Raman measurements showed increased lysosomal activity around the nanoplatforms. These results were published in the journal Biomaterials Science (Royal Society of Chemistry) [51].

To conclude, the application of bioconjugated MoS<sub>2</sub> based nanoplatform as a next-generation low-toxicity platform for selective drug delivery and treatment system was demonstrated.



The presented work consolidated the tasks given by the original assignment of my PhD project:

- Langmuir layers of  $\text{MoS}_2$  were studied, and a planar test model was created for the optimization of the  $\text{MoS}_2$  functionalization, using in situ ellipsometry with a microfluidic cell;
- functionalized  $\text{MoS}_2$  solutions were prepared and tested, the internalization of the nanoplatform across cell membrane was followed up with different techniques (CLSM, CRM);
- the obtained results were published.

## List of publications

### Articles

1. **Tailored Langmuir-Schaefer Deposition of Few-Layer MoS<sub>2</sub> Nanosheet Films for Electronic Applications.** A. Kalosi, M. Demydenko, M. Bodik, J. Hagara, M. Kotlar, D. Kostiuik, Y. Halahovets, K. Vegso, A. M. Roldan, G. Singh Maurya, M. Angus, P. Veis, M. Jergel, E. Majkova, P. Siffalovic, LANGMUIR 35, 30, pp. 9802-9808, DOI: 10.1021/acs.langmuir.9b01000 (JUL 30, **2019**)

2. **Functionalized graphene transistor for ultrasensitive detection of carbon quantum dots.** J. Brndiarova, P. Siffalovic, M. Hulman, A. Kalosi, M. Bodik, V. Skakalova, M. Micusik, Z. Markovic, E. Majkova, K. Frohlich, J. Appl. Phys. 126, 214303, DOI: 10.1063/1.5120757 (DEC 4, **2019**)

3. **A bioconjugated MoS<sub>2</sub> based nanoplatform with increased binding efficiency to cancer cells.** A. Kálosi, M. Labudová, A. Annušová, M. Benkovičová, M. Bodík, J. Kollár, M. Kotlár, P. Kasak, M. Jergel, S. Pastoreková, P. Siffalovic, E. Majkova, Biomater Sci 8(7):1973-1980. DOI: 10.1039/c9bm01975h (Mar 31, **2020**)

### Conference proceedings

1. **On the feasibility of application of bio-conjugated MoS<sub>2</sub> based nanoplatform for targeted cancer treatment.** A. Kalosi, A.

Annusova, M. Labudova, N. Bugarova, M.E. Sohova, M. Benkovicova, M. Bodik, M. Jergel, P. Siffalovic, E. Majkova, M. Omastova, S. Pastorekova, NANOCON 2018 - Conference Proceedings, 10th Anniversary International Conference on Nanomaterials - Research and Application, pp. 318-323, **2019**

**2. Towards a functionalized MoS<sub>2</sub> nanoplatform design for antibody mediated cancer therapy.** A. Kalosi, M. Benkovicova, M. Bodik, A. Annušova, M. Jergel, P. Siffalovic, E. Majkova, ELITECH '18, 20th Conference of Doctoral Students, 23 May, **2018**, FEI STU, Bratislava, Slovakia

#### **Poster contributions**

**1. Partial Zwitterionic Coating on MoS<sub>2</sub> Nanoplatfroms for Non-Specific Cellular Uptake Regulation.** A. Kálosi, M. Labudová, A. Annušová, M. Benkovičová, J. Kollár, M. Jergel, P. Siffalovic, E. Majkova, Graphene 2019, Rome, June 25-29, **2019**

**2. Biomodified nanoplatfroms for cancer targeting.** In 16th European Conference on Organized Films, N. Bugárová, M. Bodík, A. Kálosi, A. Annušová, P. Šiffalovič, I. Kajanová, J. Kollár, Zdenko Špitálsky, M. Mičušík, M. Omastová, 16th European Conference on Organized Films ECOF 16, Paris, France: Université Paris Descartes, **2019**

**3. Towards antibody mediated bio-sensing by means of immobilized MoS<sub>2</sub> nanoflakes.** A. Kálosi, M. Bodik, P. Siffalovic, M. Demydenko, Y. Halahovets, D. Kostiuk, M. Jergel, Eva Majkova, Graphene 2017, Barcelona, March 28-31, **2017**

**4. Bio-conjugation of self-assembled and deposited MoS<sub>2</sub> layers for bio-sensing applications.** A. Kalosi, M. Bodik, P. Siffalovic, M. Jergel, D. Chi, E. Majkova, 15th European Conference on Organized Films ECOF 15, Dresden, July 17 –20, **2017**

## Bibliography

- [1] X. Huang and M. A. El-sayed, "Gold nanoparticles : Optical properties and implementations in cancer diagnosis and photothermal therapy," *J. Adv. Res.*, vol. 1, pp. 13–28, 2010.
- [2] S. D. Anderson, V. V. Gwenin, and C. D. Gwenin, "Magnetic Functionalized Nanoparticles for Biomedical, Drug Delivery and Imaging Applications," *Nanoscale Res. Lett.*, vol. 14, no. 1, p. 188, May 2019.
- [3] N. Bugárová *et al.*, "A Multifunctional Graphene Oxide Platform for Targeting Cancer," *Cancers (Basel)*, vol. 11, no. 6, p. 753, May 2019.
- [4] C.-M. J. Hu *et al.*, "Half-Antibody Functionalized Lipid-Polymer Hybrid Nanoparticles for Targeted Drug Delivery to Carcinoembryonic Antigen Presenting Pancreatic Cancer Cells," *Mol. Pharm.*, vol. 7, no. 3, pp. 914–920, Jun. 2010.
- [5] M. Zhu *et al.*, "Physicochemical Properties Determine Nanomaterial Cellular Uptake, Transport, and Fate," *Acc. Chem. Res.*, vol. 46, no. 3, pp. 622–631, Mar. 2013.
- [6] C. Graf *et al.*, "Shape-Dependent Dissolution and Cellular Uptake of Silver Nanoparticles," *Langmuir*, vol. 34, no. 4, pp. 1506–1519, Jan. 2018.
- [7] B. D. Chithrani, A. A. Ghazani, and W. C. W. Chan, "Determining the size and shape dependence of gold nanoparticle uptake into mammalian cells," *Nano Lett.*, vol. 6, no. 4, pp. 662–668, Apr. 2006.
- [8] K. P. García *et al.*, "Zwitterionic-coated 'stealth' nanoparticles for biomedical applications: Recent advances in countering biomolecular corona formation and uptake by the mononuclear phagocyte system," *Small*, vol. 10, no. 13, pp. 2516–2529, 2014.
- [9] J. V. Jokerst, T. Lobovkina, R. N. Zare, and S. S. Gambhir, "Nanoparticle PEGylation for imaging and therapy," *Nanomedicine*, vol. 6, no. 4, pp. 715–728, Jun. 2011.
- [10] A. Kumar *et al.*, "Biomaterials Gold nanoparticles functionalized with therapeutic and targeted peptides for cancer treatment," *Biomaterials*, vol. 33, no. 4, pp. 1180–1189, 2012.
- [11] Y. Li, Y. Gao, C. Gong, and Z. Wang, "A33 antibody-functionalized

- exosomes for targeted delivery of doxorubicin against colorectal cancer," *Nanomedicine Nanotechnology, Biol. Med.*, vol. 14, no. 7, pp. 1973–1985, 2018.
- [12] A. Kalosi *et al.*, "On the feasibility of application of bio-conjugated mos2 based nanoplatform for targeted cancer treatment," in *NANOCON 2018 - Conference Proceedings, 10th Anniversary International Conference on Nanomaterials - Research and Application*, 2019, pp. 318–323.
- [13] M. Hadi, H. Amani, A. Akbar, H. Pazoki-toroudi, and B. Sedighimoghaddam, "Various methods of gold nanoparticles ( GNPs ) conjugation to antibodies," *Sens. Bio-Sensing Res.*, vol. 9, pp. 17–22, 2016.
- [14] K. S. Novoselov *et al.*, "Electric Field Effect in Atomically Thin Carbon Films," *Science (80-. )*, vol. 306, no. 5696, pp. 666–669, 2004.
- [15] H. Q. Bao *et al.*, "Chitosan-Functionalized Graphene Oxide as a Nanocarrier for Drug and Gene Delivery," *Small*, vol. 7, no. 11, pp. 1569–1578, 2011.
- [16] X. J. Fan, G. Z. Jiao, W. Zhao, P. F. Jin, and X. Li, "Magnetic Fe3O4-graphene composites as targeted drug nanocarriers for pH-activated release," *Nanoscale*, vol. 5, no. 3, pp. 1143–1152, 2013.
- [17] H. Zhang, "Introduction: 2D Materials Chemistry," *Chem. Rev.*, vol. 118, no. 13, pp. 6089–6090, Jul. 2018.
- [18] Y. Chen, C. L. Tan, H. Zhang, and L. Z. Wang, "Two-dimensional graphene analogues for biomedical applications," *Chem. Soc. Rev.*, vol. 44, no. 9, pp. 2681–2701, 2015.
- [19] S. S. Chou *et al.*, "Chemically exfoliated MoS2 as near-infrared photothermal agents," *Angew Chem Int Ed Engl*, vol. 52, no. 15, pp. 4160–4164, 2013.
- [20] W. Feng *et al.*, "Flower-like PEGylated MoS2 nanoflakes for near-infrared photothermal cancer therapy," *Sci Rep*, vol. 5, p. 17422, 2015.
- [21] S. G. Wang *et al.*, "Biocompatible PEGylated MoS2 nanosheets: Controllable bottom-up synthesis and highly efficient photothermal regression of tumor," *Biomaterials*, vol. 39, pp. 206–217, 2015.
- [22] J. Yu *et al.*, "Smart MoS2/Fe3O4 Nanotheranostic for Magnetically

# STU

- Targeted Photothermal Therapy Guided by Magnetic Resonance/Photoacoustic Imaging," *Theranostics*, vol. 5, no. 9, pp. 931–945, 2015.
- [23] T. Liu *et al.*, "Combined photothermal and photodynamic therapy delivered by PEGylated MoS<sub>2</sub> nanosheets," *Nanoscale*, vol. 6, no. 19, pp. 11219–11225, 2014.
- [24] J. N. Coleman *et al.*, "Two-Dimensional Nanosheets Produced by Liquid Exfoliation of Layered Materials," *Science (80-. )*, vol. 331, no. 6017, pp. 568–571, 2011.
- [25] C. Backes *et al.*, "Guidelines for Exfoliation, Characterization and Processing of Layered Materials Produced by Liquid Exfoliation," *Chem. Mater.*, vol. 29, no. 1, pp. 243–255, Jan. 2017.
- [26] A. Kalosi *et al.*, "Tailored Langmuir-Schaefer Deposition of Few-Layer MoS<sub>2</sub> Nanosheet Films for Electronic Applications," *Langmuir*, vol. 35, no. 30, pp. 9802–9808, 2019.
- [27] K.-G. Zhou, N.-N. Mao, H.-X. Wang, Y. Peng, and H.-L. Zhang, "A Mixed-Solvent Strategy for Efficient Exfoliation of Inorganic Graphene Analogues," *Angew. Chemie Int. Ed.*, vol. 50, no. 46, pp. 10839–10842, 2011.
- [28] C. Backes *et al.*, "Production of Highly Monolayer Enriched Dispersions of Liquid-Exfoliated Nanosheets by Liquid Cascade Centrifugation," *ACS Nano*, vol. 10, no. 1, pp. 1589–1601, Jan. 2016.
- [29] A. O'Neill, U. Khan, and J. N. Coleman, "Preparation of High Concentration Dispersions of Exfoliated MoS<sub>2</sub> with Increased Flake Size," *Chem. Mater.*, vol. 24, no. 12, pp. 2414–2421, Jun. 2012.
- [30] Y. Li, X. Yin, and W. Wu, "Preparation of Few-Layer MoS<sub>2</sub> Nanosheets via an Efficient Shearing Exfoliation Method," *Ind. Eng. Chem. Res.*, vol. 57, no. 8, pp. 2838–2846, Feb. 2018.
- [31] A. Jawaid *et al.*, "Mechanism for Liquid Phase Exfoliation of MoS<sub>2</sub>," *Chem. Mater.*, vol. 28, no. 1, pp. 337–348, Jan. 2016.
- [32] H. Ma, Z. Shen, and S. Ben, "Understanding the exfoliation and dispersion of MoS<sub>2</sub> nanosheets in pure water," *J. Colloid Interface Sci.*, vol. 517, pp. 204–212, 2018.
- [33] J. Kim *et al.*, "Direct exfoliation and dispersion of two-dimensional

- materials in pure water via temperature control," *Nat. Commun.*, vol. 6, no. 1, p. 8294, 2015.
- [34] H. Ma, Z. Shen, and S. Ben, "Surfactant-free exfoliation of multilayer molybdenum disulfide nanosheets in water," *J. Colloid Interface Sci.*, vol. 537, pp. 28–33, 2019.
- [35] V. Forsberg *et al.*, "Exfoliated MoS(2) in Water without Additives," *PLoS One*, vol. 11, no. 4, p. e0154522, 2016.
- [36] X. Hai *et al.*, "Engineering the Edges of MoS2 (WS2) Crystals for Direct Exfoliation into Monolayers in Polar Micromolecular Solvents," *J. Am. Chem. Soc.*, vol. 138, no. 45, pp. 14962–14969, Nov. 2016.
- [37] E. P. Nguyen *et al.*, "Electronic Tuning of 2D MoS2 through Surface Functionalization," *Adv Mater*, vol. 27, no. 40, pp. 6225–6229, 2015.
- [38] S. Kc, R. C. Longo, R. Addou, R. M. Wallace, and K. Cho, "Impact of intrinsic atomic defects on the electronic structure of MoS2 monolayers," *Nanotechnology*, vol. 25, no. 37, pp. 1–6, 2014.
- [39] T. Liu *et al.*, "Drug Delivery with PEGylated MoS2 Nano-sheets for Combined Photothermal and Chemotherapy of Cancer," *Adv. Mater.*, vol. 26, no. 21, pp. 3433–3440, 2014.
- [40] M. Wilchek and E. A. Bayer, "The avidin-biotin complex in immunology," *Immunol. Today*, vol. 5, no. 2, pp. 39–43, 1984.
- [41] M. Wilchek and E. A. Bayer, "The avidin-biotin complex in bioanalytical applications," *Anal. Biochem.*, vol. 171, no. 1, pp. 1–32, 1988.
- [42] P. C. Trippier, "Synthetic Strategies for the Biotinylation of Bioactive Small Molecules," *ChemMedChem*, vol. 8, no. 2, pp. 190–203, 2013.
- [43] S. A. Sundberg, R. W. Barrett, M. Pirrung, A. L. Lu, B. Kiangsoontra, and C. P. Holmes, "Spatially-Addressable Immobilization of Macromolecules on Solid Supports," *J. Am. Chem. Soc.*, vol. 117, no. 49, pp. 12050–12057, 1995.
- [44] C. L. Smith, J. S. Milea, and G. H. Nguyen, "Immobilization of Nucleic Acids Using Biotin-Strept(avidin) Systems," in *Immobilisation of DNA on Chips II*, C. Wittmann, Ed. Berlin, Heidelberg: Springer Berlin Heidelberg, 2005, pp. 63–90.
- [45] S. Q. Hutsell, R. J. Kimple, D. P. Siderovski, F. S. Willard, and A. J. Kimple,

- “High-Affinity Immobilization of Proteins Using Biotin- and GST-Based Coupling Strategies,” in *Surface Plasmon Resonance: Methods and Protocols*, N. J. Mol and M. J. E. Fischer, Eds. Totowa, NJ: Humana Press, 2010, pp. 75–90.
- [46] S. Pastorekova, Z. Zavadova, M. Kostal, O. Babusikova, and J. Zavada, “A novel quasi-viral agent, MaTu, is a two-component system,” *Virology*, vol. 187, no. 2, pp. 620–626, 1992.
- [47] J. Pastorek *et al.*, “Cloning and characterization of MN, a human tumor-associated protein with a domain homologous to carbonic anhydrase and a putative helix-loop-helix DNA binding segment,” *Oncogene*, vol. 9, no. 10, pp. 2877–2888, 1994.
- [48] V. Hovanky and K. Mehta, “Carbonic Anhydrase IX Inhibitors : Finding Potential Therapeutic Cancer Agents Through Virtual Screening,” *J. Young Investig.*, vol. 27, no. 2, pp. 1–10, 2014.
- [49] V. Alterio *et al.*, “Crystal structure of the catalytic domain of the tumor-associated human carbonic anhydrase IX.,” *Proc. Natl. Acad. Sci. U. S. A.*, vol. 106, no. 38, pp. 16233–16238, Sep. 2009.
- [50] N. Robertson, C. Potter, and A. L. Harris, “Role of carbonic anhydrase IX in human tumor cell growth, survival, and invasion.,” *Cancer Res.*, vol. 64, no. 17, pp. 6160–6165, Sep. 2004.
- [51] A. Kálosi *et al.*, “A bioconjugated MoS2 based nanoplatform with increased binding efficiency to cancer cells,” *Biomater. Sci.*, vol. 8, no. 7, pp. 1973–1980, 2020.
- [52] J. Pastorek, S. Pastorekova, and M. Zatovicova, “Cancer-Associated Carbonic Anhydrases and Their Inhibition,” *Curr. Pharm. Des.*, vol. 14, no. 7, pp. 685–698, 2008.
- [53] C. Lee, H. Yan, L. E. Brus, T. F. Heinz, J. Hone, and S. Ryu, “2010, C Lee, Anomalous Lattice Vibrations of Singleand Few-Layer MoS2.pdf,” *ACS Nano*, vol. 4, no. 5, pp. 2695–2700, 2010.
- [54] D. M. Carey, “Measurement of the Raman spectrum of liquid water,” *J. Chem. Phys.*, vol. 108, no. 7, pp. 2669–2675, 1998.
- [55] N. K. Howell, G. Arteaga, S. Nakai, and E. C. Y. Li-Chan, “Raman spectral analysis in the C - H stretching region of proteins and amino acids for investigation of hydrophobic interactions,” *J. Agric. Food Chem.*, vol. 47, no. 3, pp. 924–933, 1999.

# STU

- [56] B. Prats Mateu *et al.*, "Label-free live cell imaging by Confocal Raman Microscopy identifies CHO host and producer cell lines," *Biotechnol. J.*, vol. 12, no. 1, pp. 1600037(1–8), Jan. 2017.
- [57] C. Krafft, T. Knetschke, A. Siegner, R. H. W. Funk, and R. Salzer, "Mapping of single cells by near infrared Raman microspectroscopy," *Vib. Spectrosc.*, vol. 32, no. 1 SPEC., pp. 75–83, 2003.
- [58] A. Kalosi *et al.*, "Towards a functionalized MoS<sub>2</sub> nanoplatform design for antibody mediated cancer therapy," in *ELITECH'18*, 2018, no. May, pp. 2–5.
- [59] X. Wang *et al.*, "Differences in the Toxicological Potential of 2D versus Aggregated Molybdenum Disulfide in the Lung," *Small*, vol. 11, no. 38, pp. 5079–5087, 2015.
- [60] E. L. K. Chng, Z. Sofer, and M. Pumera, "MoS<sub>2</sub> exhibits stronger toxicity with increased exfoliation," *Nanoscale*, vol. 6, no. 23, pp. 14412–14418, 2014.
- [61] J. H. Appel *et al.*, "Low Cytotoxicity and Genotoxicity of Two-Dimensional MoS<sub>2</sub> and WS<sub>2</sub>," *ACS Biomater. Sci. Eng.*, vol. 2, no. 3, pp. 361–367, 2016.
- [62] X. Zhu *et al.*, "Intracellular Mechanistic Understanding of 2D MoS<sub>2</sub>Nanosheets for Anti-Exocytosis-Enhanced Synergistic Cancer Therapy," *ACS Nano*, vol. 12, no. 3, pp. 2922–2938, 2018.
- [63] L. Jia *et al.*, "Aptamer loaded MoS<sub>2</sub> nanoplates as nanoprobe for detection of intracellular ATP and controllable photodynamic therapy," *Nanoscale*, vol. 7, no. 38, pp. 15953–15961, 2015.
- [64] J. Kaur *et al.*, "Biological interactions of biocompatible and water-dispersed MoS<sub>2</sub> nanosheets with bacteria and human cells," *Sci. Rep.*, vol. 8, no. 1, p. 16386, 2018.
- [65] A. Adan, G. Alizada, Y. Kiraz, Y. Baran, and A. Nalbant, "Flow cytometry: basic principles and applications.," *Crit. Rev. Biotechnol.*, vol. 37, no. 2, pp. 163–176, 2017.
- [66] B. D. Grant and J. G. Donaldson, "Pathways and mechanisms of endocytic recycling," *Nat. Rev. Mol. Cell Biol.*, vol. 10, no. 9, pp. 597–608, Sep. 2009.
- [67] A. Christina *et al.*, "Biodistribution and pharmacokinetics of 125I-

# STU

labeled monoclonal antibody M75 specific for carbonic anhydrase IX, an intrinsic marker of hypoxia, in nude mice xenografted with human colorectal carcinoma," *Int. J. Cancer*, vol. 105, no. 6, pp. 873–881, Jul. 2003.